

## Superconductivity: A testing ground for models of confinement

James S. Ball and Ariel Caticha

*Physics Department, University of Utah, Salt Lake City, Utah 84112*

(Received 13 July 1987)

The interaction of a magnetic monopole-antimonopole pair in a superconductor is calculated as a function of their separation and the value of the Landau-Ginzburg parameter. This direct numerical result is then compared to the bag approximation to the same interaction in a superconducting medium. The actual potential exhibits the same general features as those obtained in the bag calculation. If the bag pressure is used as a phenomenological parameter, rather than the value fixed by the superconducting energy density, the agreement is excellent. Numerically the actual problem was actually no more difficult than the bag calculation. The interaction between magnetic monopoles and antimonopoles in the superconducting vacuum state is similar to the interaction of heavy colored quarks in a flux-confining physical QCD vacuum state. This means that our results are probably a good indication of the general behavior of the QCD potential and of the reliability of the bag approximation in the calculation of this potential. Our results also show that the bag model is a good approximation to a dual superconductor. This indicates that a dual superconducting picture of QCD would lead to the same heavy-quark potential and perhaps retain more of the physics than the bag model.

### I. INTRODUCTION

A superconductor is a real, well-understood physical system in which flux confinement occurs because of the presence of a nonperturbative vacuum state. If a monopole-antimonopole pair in a superconducting medium is separated, a tube of quantized magnetic flux will form which carries the flux from the monopole to the antimonopole. At large distances this flux tube yields a long-range pair potential that grows linearly with distance. This behavior is quite similar to what is believed to be the interaction of quarks in QCD where tubes of quantized color-electric flux are expected to form between distant heavy quarks, leading again to a potential which grows linearly with separation.

This similarity between superconductivity and QCD was first pointed out by Nielsen and Olesen<sup>1</sup> and by Nambu<sup>2</sup> and was used to investigate the stringlike structures connecting colored quarks (the zero-radius limit of tubes of color flux). Exploiting the QCD superconductor analogy, Mandelstam<sup>3</sup> and 't Hooft<sup>4</sup> pointed out that color-electric vector potentials can be defined in QCD (thereby perhaps identifying the dynamical variables appropriate to the study of confinement) and that chromomagnetic monopoles might play a role analogous to the Cooper pairs of superconductivity. More recently, a dual superconductor picture of QCD was proposed by Nair and Rosenzweig<sup>5</sup> and an effective dual variable Lagrangian for QCD was constructed by Baker, Ball, and Zachariasen<sup>6</sup> based on an analysis of the behavior of the QCD Green's functions. This Lagrangian, which may be considered the analog of the Landau-Ginzburg approach to superconductivity, successfully accounts for the formation of tubes of quantized color-electric flux.

Alcock, Burfitt, and Cottingham<sup>7</sup> have proposed that the solution of the Landau-Ginzburg equations for monopoles might be used directly to provide a phenome-

nological model for the potential between heavy quarks and showed that qualitatively correct behavior could be obtained. In this work we will focus on studying in detail the behavior of monopoles in a superconductor to determine how the interaction with the nonperturbative vacuum changes the short-range Coulomb potential to a linearly rising long-range potential. This is an interesting theoretical problem in its own right. In addition, by simply dividing the superconductor into regions of normal material (perturbative vacuum) and superconducting material (nonperturbative vacuum) a simple bag approximation can be obtained which is identical to the MIT bag model used in the calculation of the potential between heavy quarks. In other words, not only can we obtain an exact confining potential calculated directly from first principles but we can also construct its bag approximation. This allows us to test the accuracy and applicability of the bag approximation.

The organization of this paper is as follows. In Sec. II we will develop the formalism necessary to include magnetic monopoles into the Landau-Ginzburg description of superconductivity. In Sec. III we discuss the numerical methods used in solving the field equations. Section IV contains the derivation of the bag approximation and the numerical methods used to solve it and a comparison of the numerical results of the exact solution with those of the bag approximation. In Sec. V the results and a scaling method suggested by the bag model which allows one to obtain the potential for a wide range of the Landau-Ginzburg parameter from the solution at a single value are discussed.

### II. HEAVY MONOPOLES IN A LANDAU-GINZBURG SUPERCONDUCTOR

The usual definition of  $\mathbf{B}$  in terms of the vector potential  $\mathbf{A}$  automatically implies the absence of magnetic

monopoles, i.e.,  $\nabla \cdot \mathbf{B} = 0$ . Following Dirac (see Ref. 8) we introduce sources of magnetic flux of modifying the relation between  $\mathbf{B}$  and  $\mathbf{A}$  as

$$\mathbf{B} = \nabla \times \mathbf{A} + \mathbf{B}_s, \quad (2.1)$$

and choose the "string field"  $\mathbf{B}_s$  to satisfy

$$\nabla \cdot \mathbf{B}_s = \rho_m.$$

Thus  $\mathbf{B}$  satisfies Gauss's law with a magnetic source. For a single monopole in vacuum located at the origin, Eq. (2.1) simply reflects the identity (in spherical coordinates)

$$\frac{\hat{\mathbf{r}}}{4\pi r^2} = -\nabla \times \left[ \frac{1 + \cos\theta}{4\pi r \sin\theta} \right] \hat{\boldsymbol{\phi}} + \delta(x)\delta(y)\theta(z)\hat{\mathbf{z}}. \quad (2.2)$$

In this case the string field  $\mathbf{B}_s$  is

$$\mathbf{B}_s = \delta(x)\delta(y)\theta(z)\hat{\mathbf{z}}. \quad (2.3)$$

This field exists only along the positive  $z$  axis and serves to cancel the string in  $\nabla \times \mathbf{A}$  which results from the attempt to represent a point charge as the curl of something. Both  $\nabla \times \mathbf{A}$  and  $\mathbf{B}_s$  contain strings while  $\mathbf{B}$  does not, as is required on physical grounds. The vector potential that represents the magnetic field produced by a monopole-antimonopole pair located on the  $z$  axis at  $z = \pm R/2$  is

$$\mathbf{A} = A_D \hat{\boldsymbol{\phi}} = -\frac{q}{4\pi\rho} \left[ \frac{z - R/2}{[\rho^2 + (z - R/2)^2]^{1/2}} - \frac{z + R/2}{[\rho^2 + (z + R/2)^2]^{1/2}} \right] \hat{\boldsymbol{\phi}}, \quad (2.4)$$

where we have shifted to cylindrical coordinates which will be used in our numerical calculations and where  $q$  is the magnetic charge. The associated  $\mathbf{B}_s$  is

$$\mathbf{B}_s = +q\delta(x)\delta(y)[\theta(z - R/2) - \theta(z + R/2)]\hat{\mathbf{z}}, \quad (2.5)$$

and the string now joins the two magnetic charges.

The time-independent Landau-Ginzburg (LG) action in the presence of these sources is identical to the usual LG action with the modified relationship

$$L_{\text{LG}} = - \int d^3x \left[ \frac{1}{2} B^2 - \phi^* (\nabla - ie\mathbf{A})^2 \phi + \lambda (|\phi|^2 - |\phi_0|^2)^2 \right]. \quad (2.6)$$

Here  $\phi$  is the order parameter (the scalar field in the Abelian Higgs model) and  $e$  is the scalar field charge; in a real superconductor this is the charge of a Cooper pair, twice the electron charge.

The Dirac quantization condition  $eq = 2\pi$  ensures that the location of the string can be changed by a gauge transformation and, therefore, that the strings are unobservable. Having the string connect the two magnetic charges is a convenient gauge choice for our calculation in that it will require the vector potential to vanish exponentially at large distances from the monopole-antimonopole pair. Finally, we write

$$\mathbf{A} = \mathbf{A}_D + \mathbf{a}, \quad (2.7)$$

where  $\mathbf{A}_D$  produces the field of the monopoles in vacuum with the associated strings and  $\mathbf{a}$  and  $\nabla \times \mathbf{a}$  are well behaved everywhere in space and have as a source the current produced by the  $\phi$  field. This not only eliminates Coulomb and string singularities from the field equations for the new independent variable  $\mathbf{a}$  but allows easy separation of the infinite monopole self-energy from the total energy. This is accomplished by using the identity

$$\int d^3x \frac{1}{2} (\nabla \times \mathbf{A}_D + \mathbf{B}_s)^2 = -\frac{q^2}{4\pi R} + \text{self-energy}. \quad (2.8)$$

Since the sources have axial symmetry, we make the following field ansatz:

$$a_0 = 0, \quad \mathbf{a} = a(\rho, z)\hat{\boldsymbol{\phi}}, \quad \text{and} \quad \phi = \phi^* = \phi(\rho, z). \quad (2.9)$$

The vector potential is then in Coulomb gauge and the choice of string direction and the large-distance behavior of  $\mathbf{A}$  allows  $\phi$ , the scalar field, to be real. The resulting field equations are

$$[\nabla^2 - e^2(a + A_D)^2]\phi = 2\lambda(\phi^2 - \phi_0^2)\phi \quad (2.10)$$

and

$$\left[ \nabla^2 - \frac{1}{\rho^2} \right] a = 2e^2(a + A_D)\phi^2. \quad (2.11)$$

It should be noted that in certain physically realizable situations we expect the minimum-energy solution to exhibit spontaneous symmetry breaking and to lie outside of our simple ansatz. This will be discussed in more detail in Sec. V.

In terms of these functions, the total field energy, dropping the monopole self-energies, can be written as

$$E = -\frac{\pi}{e^2 R} + \int d^3x [\lambda(\phi_0^4 - \phi^4) - e^2\phi^2(a + A_D)a]. \quad (2.12)$$

Here we have made use of the field equations and the Dirac quantization condition to simplify this expression.

There are two length scales in superconductivity. These are the penetration depth  $\lambda(T)$ , which controls the exponential rate of change of the vector potential, and the coherence length  $\xi(T)$ , which controls the rate at which  $\phi$  approaches  $\phi_0$ . These are related to the photon mass and the Higgs scalar mass in the superconducting states and are the following functions of our parameters:

$$m_A = 1/\lambda(T) = \sqrt{2}e\phi_0 \quad \text{and} \quad m_\phi = [\sqrt{2}\xi(T)]^{-1} \\ = 2\sqrt{\lambda}\phi_0.$$

In order to minimize the number of constants appearing in our field equations, we will rescale distance and the fields as

$$\mathbf{x} = \mathbf{x}'/m_A, \quad a = \sqrt{2}\phi_0 a', \\ A_D = \sqrt{2}\phi_0 A_D', \quad \text{and} \quad \phi = \phi_0 \phi'. \quad (2.13)$$

Dropping the primes, Eqs. (2.10), (2.11), and (2.12) become

$$\nabla^2 \phi - (a + A_D)^2 \phi = \kappa^2 \phi (\phi^2 - 1), \quad (2.14)$$

$$\nabla^2 a - \frac{a}{\rho^2} - \phi^2 (a + A_D) = 0, \quad (2.15)$$

and

$$E = \frac{\phi_0^2}{m_A} \left[ -\frac{2\pi}{R} + \int d^3x \left[ \frac{\kappa^2}{2} (1 - \phi^4) - (a + A_D) a \phi^2 \right] \right], \quad (2.16)$$

where we have introduced the Landau-Ginzburg parameter

$$\kappa = \frac{m_\phi}{\sqrt{2} m_A}. \quad (2.17)$$

We will refer to the scaled quantity in square brackets in Eq. (2.16) as the scaled interaction energy which will be related to the scaled string tension.

The boundary conditions for the scaled fields which lead to a unique solution to Eqs. (2.14) and (2.15) are that  $a$  goes to  $-A_D$  and  $\phi$  goes to 1 as either  $\rho$  or  $z$  go to infinity. These are simply the result of requiring that  $\phi$  approach the physical vacuum in the superconductor and that  $\mathbf{A}$  vanish at large distances from the monopole-antimonopole pair. The remaining boundary conditions are that function  $a$  vanishes on the  $z$  axis, while the behavior of  $\phi$  is determined by the behavior of  $A_D$  as  $\rho \rightarrow 0$ . For  $|z| < R/2$ , between the monopoles,  $A_D \sim 1/\rho$  as  $\rho$  goes to zero forcing  $\phi$  to vanish on the  $z$  axis; however, outside of this interval  $A_D$  vanishes as  $\rho \rightarrow 0$  and the radial derivative of  $\phi$  must vanish on this portion of the  $z$  axis.

In the limit of large monopole separation, the solution between the monopole-antimonopole pair will be the ordinary vortex solution with one unit of flux, though in an unconventional gauge in which the flux returns via a string that runs along the  $z$  axis rather than at infinity as in the usual gauge.

### III. NUMERICAL SOLUTIONS OF THE FIELD EQUATIONS

The axial symmetry of the problem suggests the use of cylindrical coordinates  $z$  and  $\rho$  as independent variables. Furthermore, the symmetry under  $z \rightarrow -z$  means that a complete solution can be obtained by considering only the half-space  $z > 0$  with the appropriate boundary conditions imposed on the  $z=0$  plane to guarantee this symmetry. Both  $a$  and  $\phi$  are even functions of  $z$ , as a result their boundary conditions on the  $z=0$  plane are

$$\frac{\partial \phi}{\partial z} = \frac{\partial a}{\partial z} = 0.$$

The two-dimensional area  $0 < \rho < \rho_{\max}$  and  $0 < z < z_{\max}$  is discretized on a rectangular  $n \times m$  mesh. Using the standard central difference approximations for the derivatives, the field equations become difference equations on this lattice. The fact that the dynamical fields fall with a known exponential behavior at large  $z$  and  $\rho$  allows one to estimate the values of  $\rho_{\max}$  and  $z_{\max}$  neces-

sary to produce a sufficiently accurate solution. In practice we varied these quantities to show that the quantities of physical interest, such as the string tension, were, in fact, independent of the cutoff values.

The numerical solution of the difference equations was obtained by using the Gauss-Seidel method with the successive overrelaxation (SOR) technique following the general procedures recommended by Adler and Piran.<sup>9</sup> The procedure was as follows. One began with a small lattice, typically  $8 \times 8$  with a guess for the first trial solution which was iterated until convergence was obtained. These solutions were then interpolated to provide a trial solution on a  $16 \times 16$  lattice. Once the solution on this lattice had been obtained, it in turn was used to provide a trial solution on a larger lattice. Because the trial functions on the larger lattices were close to the actual solutions, the convergence was generally quite rapid. In most cases a rectangular rather than a square lattice was used because as the monopole-antimonopole separation was increased, it was necessary to increase  $z_{\max}$ , requiring the use of more mesh points in the  $z$  than in the  $\rho$  direction to maintain a similar spacial resolution in each variable. The maximum change of the fields during a single Gauss-Seidel iteration was used as the criterion for convergence. For small lattices the iteration was repeated until the fields were stable to machine accuracy (double precision on a VAX 785). For the largest lattice, the iteration was stopped after the fields stabilized to six significant figures. For lattices with less than 10 000 lattice points this required one- to two-hundred iterations.

At each change of lattice the number of points was increased by a factor of 4. This procedure not only proved to be an efficient method of obtaining the solution for a large lattice but also gave information on the lattice-spacing dependence of the relevant physical quantities such as the monopole-antimonopole interaction energy. This information allowed us to estimate how large a lattice was necessary to provide a stable result and, in fact, could be used in a Richardson-type<sup>10</sup> extrapolation to zero-lattice spacing to obtain the continuum values for the quantities of interest.

The final step in this procedure was to vary  $z_{\max}$  and  $\rho_{\max}$  to verify that these parameters were large enough so that the interaction energy was independent of these cutoffs.

This procedure was carried out for several values of the Landau-Ginzburg parameter and for enough values of the monopole-antimonopole separation to obtain an accurate plot of the potential. The vortex solution was also obtained by the same general numerical procedure and was used to provide two checks on the monopole-antimonopole solutions. First, it was verified that the slope of the linear portion of the potential agreed with the vortex line string tension. Second, for large monopole-antimonopole separations the solutions on the medium plane were compared to the vortex solutions and found to be in excellent agreement. The value of  $\rho_{\max}$  for the vortex solution also provided a good estimate of the value of this parameter required in the monopole-antimonopole solution.

A further check on the vortex solution was provided

by the fact that the string tension can be calculated analytically at the critical value of the Landau-Ginzburg parameter  $\kappa=1/\sqrt{2}$  (the dividing line between type-I and type-II superconductors), in this case the scaled string tension for a vortex with  $N$  flux quanta is  $T_N=2\pi N$ . The numerical results with  $\rho_{\max}=12$  and the Richardson extrapolation using 8, 16, 32, and 64 uniformly distributed mesh points was  $T_1=6.2823$ , which is in error by 0.001. The value obtained with 64 mesh points was  $T_1=6.2744$ , which has about ten times the error, through the direct result certainly has more accuracy than is required for our purposes. For a vortex with 100 units of flux, the  $\rho_{\max}$  must be increased to 50 due to the much larger radius of this vortex, with the extrapolated result  $T_{100}=628.57$ , which has about the same percentage error as the flux 1 vortex calculation.

The comparison of the vortex string tension with the slope of the linear potential obtained from the monopole-antimonopole solution indicates that the potential is accurate to 0.1 to 0.2 in scaled units, which corresponds to an error of the order of a percent or two in the potential in that region. The fact that the potential passes through zero of course prevents us from assigning an overall percentage error, but we believe that the potential is determined at least as accurately as the bag-model potential, which will be discussed in Sec. IV.

The behavior of a typical solution (monopole-antimonopole separation  $R=6$  and  $\kappa=0.7071$ ) is shown in Figs. 1 and 2. In Fig. 1 one quadrant is shown with the  $\mathbf{B}$  field lines which leave the monopole at equally spaced angles. For comparison we have also plotted the "dipole" field lines that would exist in the absence of the superconductor. In Fig. 2 lines of constant  $\phi$  for  $\phi=0.1$  to 0.9 at intervals of 0.1 are shown to give an indication of how the  $\mathbf{B}$  field changes the nature of the vacuum states in the region of the monopole-antimonopole pair. It should be noted that already at this separation, the fields on the median plane are nearly indistinguishable

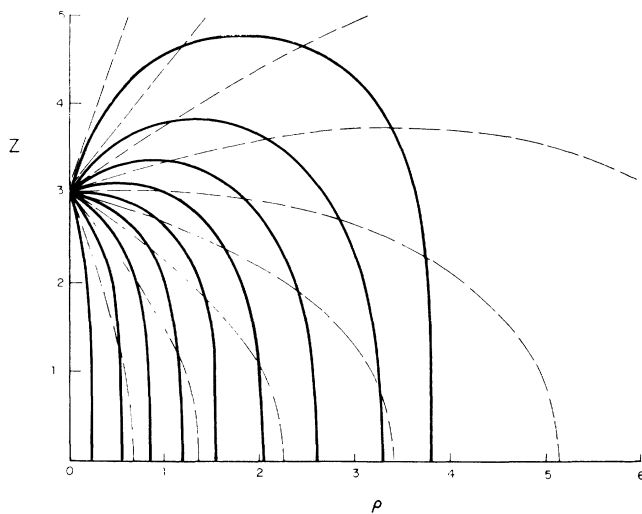


FIG. 1. The solid curves are  $\mathbf{B}$ -field lines for  $R=6.0$  and  $\kappa=0.7071$ . The dashed lines are the  $\mathbf{B}$ -field lines for  $R=6.0$  in free space.

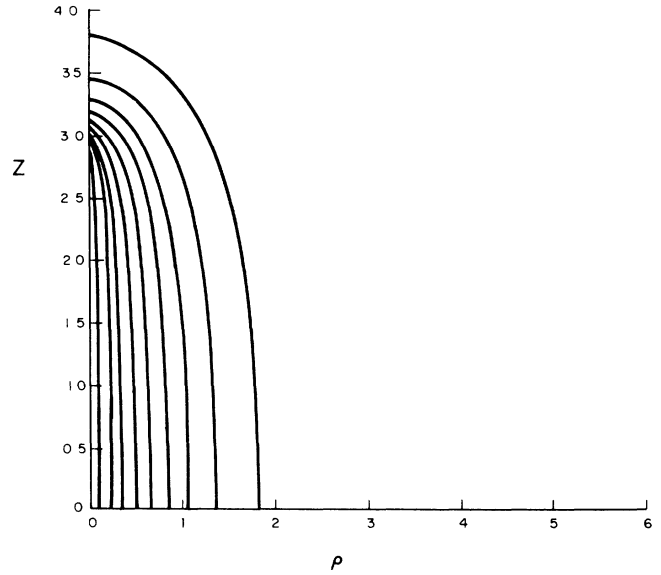


FIG. 2. Lines of constant  $\phi=0.1$  through 0.9 for  $R=6.0$  and  $\kappa=0.7071$ .

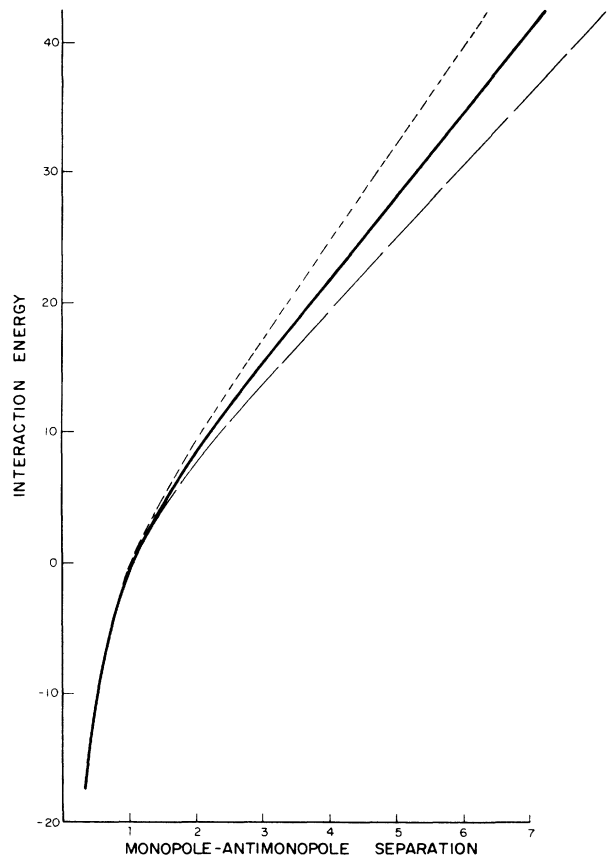


FIG. 3. Interaction energy as a function of  $R$  and  $\kappa$ . Solid line is  $\kappa=0.7071$ , long dashes represent  $\kappa=0.5$ , while short dashes represent  $\kappa=1.0$ .

from those for the one flux quantum vortex.

The resulting interaction energies for  $\kappa=0.5$ ,  $\kappa=1/\sqrt{2}$ , and for  $\kappa=1$  are shown in Fig. 3. Note the rapid change from the Coulomb region where the potentials are necessarily identical to the linear region where the different slopes are the result of the dependence of the string tension on  $\kappa$ . This rapid transition is quite similar to the "precocious scaling" observed in bag-model calculations of the heavy-quark potential.<sup>11</sup>

#### IV. BAG APPROXIMATION FOR THE MONOPOLE-ANTIMONOPOLE INTERACTION IN A SUPERCONDUCTOR

In this approach to a superconductor, space is divided into a normal region in which the magnetic field is sufficiently strong to destroy the superconductivity and a superconducting region from which the magnetic field is expelled. The basic assumption is that the volume in which the transition takes place can be approximated by a surface. It is clear from our previous discussion of the flux tube formed between the monopole-antimonopole pair that the transition occurs gradually, with a scale that is, in fact, the flux-tube radius, and that only in the extreme case of very high monopole charge or very large flux is the change sufficiently abrupt that it can justifiably be approximated by a discontinuous step. Putting aside these physical reasons for doubting the applicability of this model to our problem, we will proceed with standard bag-model calculation.

Inside the bag, the region is normal and point magnetic sources can most easily be represented by a scalar magnetic potential  $\psi$  satisfying Laplace's equations everywhere except at the sources. The boundary conditions on the surface of the bag are simply that no flux penetrates the surface,

$$\hat{\mathbf{n}} \cdot \nabla \psi = 0 \quad \text{on the surface,} \quad (4.1)$$

and that the pressure produced by the negative-energy density of the superconducting vacuum be balanced by the magnetic pressure

$$|\mathbf{B}|^2 = -2E_{\text{vac}} = 2\kappa^2 e^2 \phi_0^4, \quad (4.2)$$

where  $\mathbf{B} = -\nabla \psi$  and  $-E_{\text{vac}}$  is the usual bag constant ( $E_{\text{vac}}$  is the vacuum energy density).

The parameters that determine this model are  $E_{\text{vac}}$ , the monopole charge  $q$ , and the separation of the monopole-antimonopole pair  $R$ . Because of the way in which these parameters enter this model, it is possible to scale the length and the scalar potential  $\psi$  so that only a single parameter remains. We have chosen the following procedure:

$$\psi = \sqrt{q} (-2E_{\text{vac}})^{1/4} \bar{\psi} \quad (4.3a)$$

and

$$\mathbf{r} = \sqrt{q} (-2E_{\text{vac}})^{-1/4} \bar{\mathbf{r}}. \quad (4.3b)$$

The interaction energy is

$$E_{\text{bag}} = \int dV \left( \frac{1}{2} |\mathbf{B}|^2 - E_{\text{vac}} \right),$$

where the first term is the magnetostatic energy and the second is the energy required to create a normal region in the superconductor's negative-energy vacuum state. The interaction energy has the following relation to the scaled energy:

$$E_{\text{bag}} = (q)^{3/2} (-2E_{\text{vac}})^{1/4} \bar{E}_{\text{bag}}. \quad (4.4)$$

This scaling results in the basic problem of solving Poisson's equation with unit charges and finding the surface on which  $\mathbf{B}$  is a unit vector tangential to the surface. This procedure must be carried out for each value of the separation of the charges. The treatment of this problem is essentially that used by Baker, Ball, and Zachariasen,<sup>12</sup> which was shown to produce excellent agreement with the analytic two-dimensional bag solution of Giles.<sup>13</sup> Since we are treating a simplified version of the bag approximation of Ref. 12, we will describe the details of our calculation.

The nonlinear boundary condition on the  $\mathbf{B}$  field and the cylindrical symmetry requires the existence of cusps at each end of the bag, as well as a line charge density on the symmetry axis (the  $z$  axis in Sec. III) outside of the bag. In Ref. 12 the analytic form of these cusps were determined to be  $\rho \sim (z - z_0)^{3/2}$ , where  $z_0$  is the cusp position and the self-consistent line charge density along the axis of the cusp was proportional to  $(z - z_0)^2$ . The existence of these cusps complicate the use of cylindrical coordinates in the treatment of the bag, in that the surface  $\rho = \rho(z)$  cannot be a single-valued function of the variable  $z$ . If one attempts to simply separate the potential into  $\psi_c$ , the Coulomb potential of the two point charges, and expand the remainder in terms of the Legendre polynomial solutions to Laplace's equation, the existence of the line charges which lie outside of the bag for  $|z| > z_0$  prevents the convergence of this expansion for certain regions *inside* the bag. For this reason the potential  $\psi$  is decomposed into three parts:  $\psi_c$ , a parametrized form of the cusp potential  $\psi_{\text{cusp}}$ ; and the residual  $\psi_r$  which will have a convergent expansion inside the bag. Here, as before, we will drop the bars that denote the scaled variables in the interest of simplifying the equations. Equations (4.3) and (4.4) must, of course, be used to obtain the actual physical quantities of interest:

$$\psi = \psi_c + \psi_{\text{cusp}} + \psi_r,$$

where

$$\psi_c = -\frac{1}{4\pi} \left[ \frac{1}{|\mathbf{r} - \mathbf{r}_1|} - \frac{1}{|\mathbf{r} - \mathbf{r}_2|} \right], \quad (4.5)$$

$$\psi_{\text{cusp}} = \lambda \left[ \int_{z_0}^{z_c} \frac{(z' - z_0)^2}{[(z' - z)^2 + \rho^2]^{1/2}} dz' - \int_{-z_c}^{-z_0} \frac{(z' + z_0)^2}{[(z' - z)^2 + \rho^2]^{1/2}} dz' \right], \quad (4.6)$$

and

$$\psi_r = \sum_{l=1}^N A_l r^{2l-1} P_{2l-1}(\cos\theta). \quad (4.7)$$

Here the free parameters are the cusp position;  $z_0$ ,  $z_c$ , and  $\lambda$  which controls the length and strength of the line charges; and the  $A_1$  through  $A_N$ .

The final step in the formulation of this problem is to write an analytic expression for the bag surface as

$$r(\theta) = \frac{\sum_{l=0}^M B_l P_{2l}(\cos\theta) + C(\sin\theta)^{2/3}}{(1 + D \cos^2\theta)^{1/2}}, \quad (4.8)$$

where  $C$  and  $D$  describe the cusp shape.

Our numerical procedure is to define a positive-definite quantity

$$\chi^2 = \frac{\int dS [(\nabla\psi)^2 - 1]^2 + (\hat{n} \cdot \nabla\psi)^2}{\int dS} \quad (4.9)$$

which we minimize by varying the free parameters in  $\psi$  and the surface. The smaller  $\chi^2$ , the closer we are to the solution for which  $\chi^2=0$ . The actual procedure was as follows. We choose a surface and the parameters that enter into  $\psi_{\text{cusp}}$ . With these quantities fixed, the values of the  $A$ 's which minimize the  $(\hat{n} \cdot \mathbf{B})^2$  term in  $\chi^2$  satisfy a set of linear equations which are solved. Thus the minimization actually involves searching in the space of the surface and cusp potential parameters and determining the associated set of  $A$ 's.

Before discussing the numerical results for the interaction energy as a function of charge separation, let us examine the limit of very large separations to determine the bag-model predictions for the string tension. In our scaled units the flux tube carries one unit of flux and has  $B_z=1$ , which requires that the cross-sectional area be one. This results in a scaled energy per unit length of  $\frac{1}{2}$  from the magnetic energy and  $\frac{1}{2}$  from the bag volume energy. The scaling relation for the string tension is

$$T = q(-2E_{\text{vac}})^{1/2} \bar{T}. \quad (4.10)$$

The scaling used in Sec. III allows one to calculate all physical quantities for any value of  $e$  and  $\phi_0$  as does the bag-model scaling. For purposes of comparison between the bag model and the numerical Landau-Ginzburg (LG) calculation, we will choose  $e=1/\sqrt{2}$  and  $\phi_0=1$  so that the scaled LG energy and length are the actual values of these quantities and then scale the bag values according to  $q=2\sqrt{2}\pi$  and  $-2E_{\text{vac}}=\kappa^2$ . Note that the bag model has no requirement of flux quantization. The resulting string tension for a flux tube with  $N$  units of flux is

$$T_N = N2\sqrt{2}\pi\kappa. \quad (4.11)$$

Surprisingly, for  $\kappa=1/\sqrt{2}$ , this is identical to the exact result.

The actual numerical calculations for the interaction energy in the bag were performed for scaled  $R$  ranging from 0.1, where the interaction is dominated by the Coulomb energy, to  $R=3$ , where the central region of the bag is quite cylindrical and the change of interaction energy with  $R$  is linear. For each value of  $R$ , 20 mesh points were used to represent the discrete values of the variable  $\cos\theta$  representing half of the surface of the bag

(here as in the previous calculation we have taken advantage of the bag symmetry about the median plane). It was found that as  $R$  increased, the number of parameters ( $B$ 's) necessary to represent the surface increased and the distribution of mesh points needed to be shifted to give an adequate representation of the surface near the ends of the bag. In each case the  $\chi^2$  as defined by Eq. (4.9) was minimized using the CERN developed minimization program MINUIT. For all values of  $R$  it was possible to obtain  $\chi^2 < 5 \times 10^{-4}$  with 0.1 and 3 having the large values. The smallest value  $\chi^2 = 6 \times 10^{-6}$  was obtained at  $R=1.34$ . This meant that better bag solutions were obtained in the more interesting transition region than in the linear or in the Coulomb-dominated regions. It should be noted that the number of trial solutions required to obtain a good result was generally quite large (at least a few thousand), meaning that the calculation of the bag interaction energy at a given  $R$  required several times the computer time needed in the Landau-Ginzburg calculation of the same quantity. On the other hand, after the bag calculation has been carried out for a range of  $R$ 's, a new solution for a different value of the Landau-Ginzburg parameter can be easily obtained using the scaling properties without any further calculation. The bag shape for  $R=1.0$  is shown in Fig. 4.

In Fig. 5 we show a comparison of the actual monopole-antimonopole interaction energy with that of the bag model for  $\kappa=1/\sqrt{2}$ . Since there is no particular reason for the finite parts of the self-energies to be the same for the LG calculation and that of the bag, we have added a constant  $=0.6$  to the bag interaction energy. The agreement is truly spectacular. In Fig. 6 we show the same comparison, though this time for  $\kappa=1$ . In this case the short-range potential is still in agreement, but at large  $R$  the two calculations are not even close. It is clear that the bag-model string tension is wrong. To illustrate what might be expected at other values of  $\kappa$  we have calculated the  $N=1$  vortex string tension as a function of  $\kappa$ , which is compared to the bag

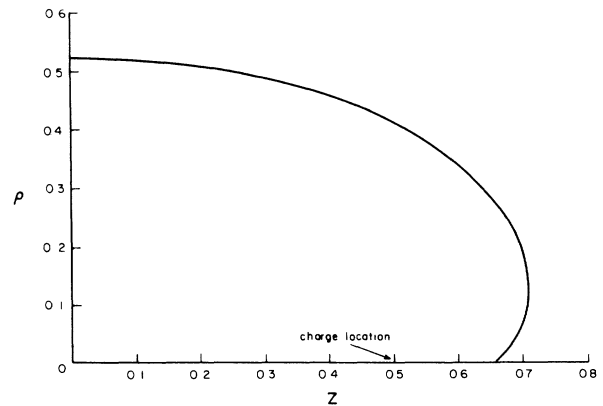


FIG. 4. Bag surface for  $R=1$ . Note that while maximum  $\rho$  and maximum  $z$  are about equal, the cusp is still a prominent feature, making this rather different from a sphere.

value in Fig. 7. Note that these curves intersect at  $\kappa=1/\sqrt{2}$ , where the surface energy associated with the superconducting normal boundary vanishes. At this point we should discuss another deficiency of the simple bag model we have studied. In a type-I superconductor, the vortex line string tension as a function of  $N$  grows at a rate less than linear, indicating that vortex lines attract one another, forming the energetically favored high-flux vortices. On the other hand, in a type-II superconductor, the string tension grows more rapidly than  $N$ , meaning that vortex lines repel and that  $N$  flux-one lines represent the lowest-energy method of passing  $N$  units of flux through a superconductor. Thus, not only is the bag-model string tension incorrect for values of  $\kappa \neq 1/\sqrt{2}$ , but the  $N$  dependence of the string tension is also wrong.

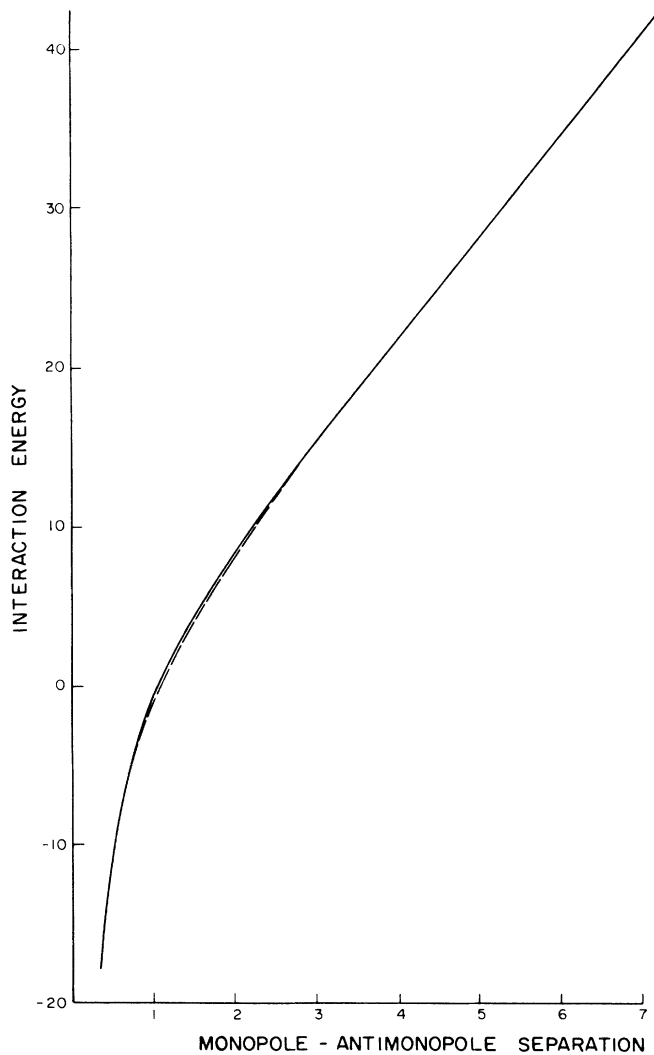


FIG. 5. Comparison of the LG interaction energy (solid line) with that obtained from the bag calculation (dashed line) for  $\kappa=0.707$ . Since a constant ( $R$  independent) difference between potentials are meaningless, we have added 0.6 to the bag results so that the portions agree.

To examine whether our failure to include the surface tension associated with the bag surface is the cause of disagreement illustrated by Fig. 6, we have calculated the surface tension as a function of  $\kappa$  for a Landau-Ginzburg superconductor. This is a one-dimensional problem and simpler than the string tension calculation. Our geometry is as follows. All fields will be assumed to be functions of the  $z$  coordinate, with large negative  $z$  being the superconducting region with  $\phi=\phi_0$  and large positive  $z$  having the equilibrium value of the magnetic field  $B_c = \sqrt{2} \lambda \phi_0^2$ . We will choose  $\mathbf{A} = A(z)\hat{x}$  and  $\mathbf{B} = A'(z)\hat{y}$ , where primes denote  $d/dz$ .

The surface tension is simply the difference in energy per unit area that one obtains from the calculation of the energy, using the dynamical fields in the transition region, from that obtained using the asymptotic values of the fields that would apply on each side of a plane boundary dividing the normal and superconducting regions. The Hamiltonian density can be written

$$H = \frac{1}{2}(A')^2 + (\phi')^2 + e^2 A^2 \phi^2 + \lambda(\phi^2 - \phi_0^2)^2, \quad (4.12)$$

where we have defined zero energy as that in the superconducting vacuum. The fact that this Hamiltonian density is zero in the superconductor and  $B_c^2$  in the nor-

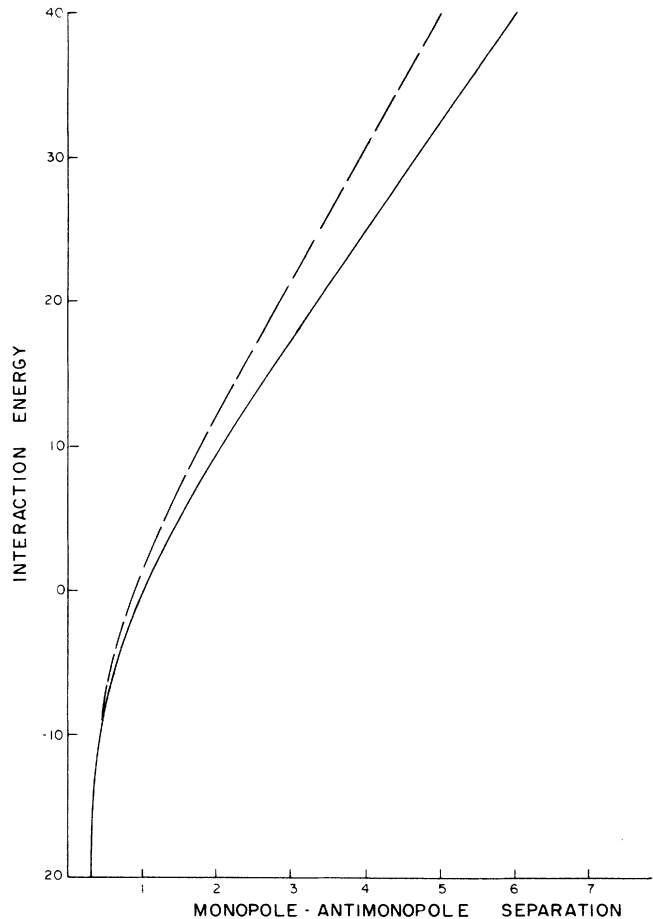


FIG. 6. Comparison of the LG interaction energy (solid line) with bag results (dashed line) for  $\kappa=1.0$ .

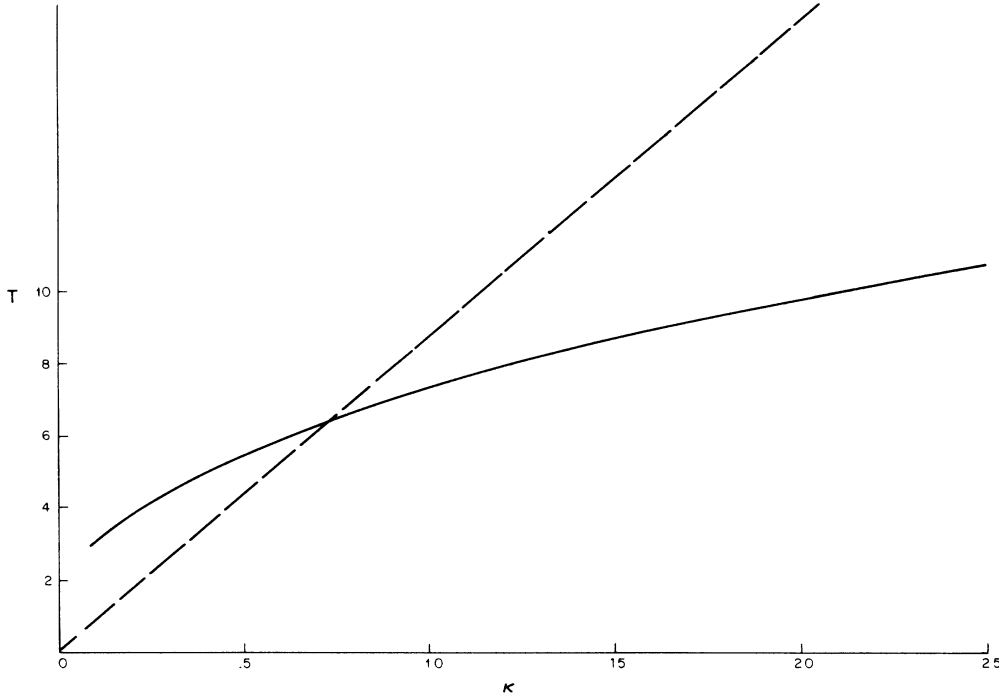


FIG. 7. String tension as a function of  $\kappa$ . LG values are the solid line, while those for the bag are the dashed line.

mal region clearly causes a problem if one naively subtracts the sharp boundary energy from the energy calculated from the dynamical fields in that shifting the position of the boundary will change the energy. It is clear that this energy associated with shifting the position of the surface has nothing to do with the surface energy which we wish to calculate. To avoid the problem of where the surface should be placed, we will employ the trick of subtracting an exact differential from  $H$  to form

$$\bar{H} = H - B_c A' . \quad (4.13)$$

Since  $A$  should satisfy the same boundary conditions at  $z \rightarrow \infty$ , this term will cancel out in the energy difference calculation. Note however that  $\bar{H}$  is continuous across the boundary and zero for all values  $z$  in the case of a sharp boundary. The surface tension  $\sigma$  is then

$$\sigma = \int_{-\infty}^{\infty} \bar{H} dz . \quad (4.14)$$

The field equations for this one-dimensional problem are

$$A'' - 2e^2 \phi^2 A = 0 \quad (4.15)$$

and

$$\phi'' - e^2 A^2 \phi - 2\lambda \phi (\phi^2 - \phi_0^2) = 0 . \quad (4.16)$$

A first integral of these equations is

$$\frac{1}{2} (A')^2 + (\phi')^2 - e^2 A^2 \phi^2 - \lambda (\phi^2 - \phi_0^2)^2 = 0 , \quad (4.17)$$

where we have used the boundary conditions at  $z = -\infty$  to evaluate this constant function (independent of  $z$ ). Evaluation of this quantity at  $z \rightarrow +\infty$  results in the pressure balance equation that determines  $B_c$ . Using

this expression or the field equations directly, the surface tension can be written

$$\sigma = \int_{-\infty}^{\infty} [-\lambda \phi^4 + \frac{1}{2} (B_c - A')^2] dz . \quad (4.18)$$

Clearly the integrand is zero except in the transition region.

In our actual calculation we use the scaling of Eq. (2.13) and calculate the scaled surface tension which is only a function of  $\kappa$ . Before showing the results, a few remarks about the boundary conditions to be used with Eqs. (4.15) and (4.16) are in order. Clearly the superconducting vacuum state with  $\phi = \phi_0$  and  $A = A' = 0$  is a  $z$ -independent solution of these equations, as is the normal state with  $A' = B_c$  and  $\phi = 0$ . This means that one must start integrating the differential equations in the region where the transition is beginning to occur. Furthermore, the values of  $A'$ ,  $A$ , and  $\phi, \phi'$  must be adjusted so that correct boundary values are obtained as  $z \rightarrow \infty$  (note that the equations can be linearized in this region fixing  $A'$  and  $\phi'$  in terms of the other two quantities). This occurs for a continuous set of starting values because the transition region is not fixed in this calculation. The fact that  $z$  does not occur in Eqs. (4.15) and (4.16) allows us to reduce the order of the system by one by introducing as the independent variable  $y = (1 - \phi)$ , where  $\phi$  is the scaled scalar field (note that  $y$  increases monotonically with  $z$ ). The use of  $y$  removes any uncertainty as to where the transition region is with reference to the  $z$  variable. The surface tension is then expressed as an integral over  $y$ . In practice the value of  $A'$  obtained as  $y \rightarrow 1$  is a very sensitive function of the input parameters.



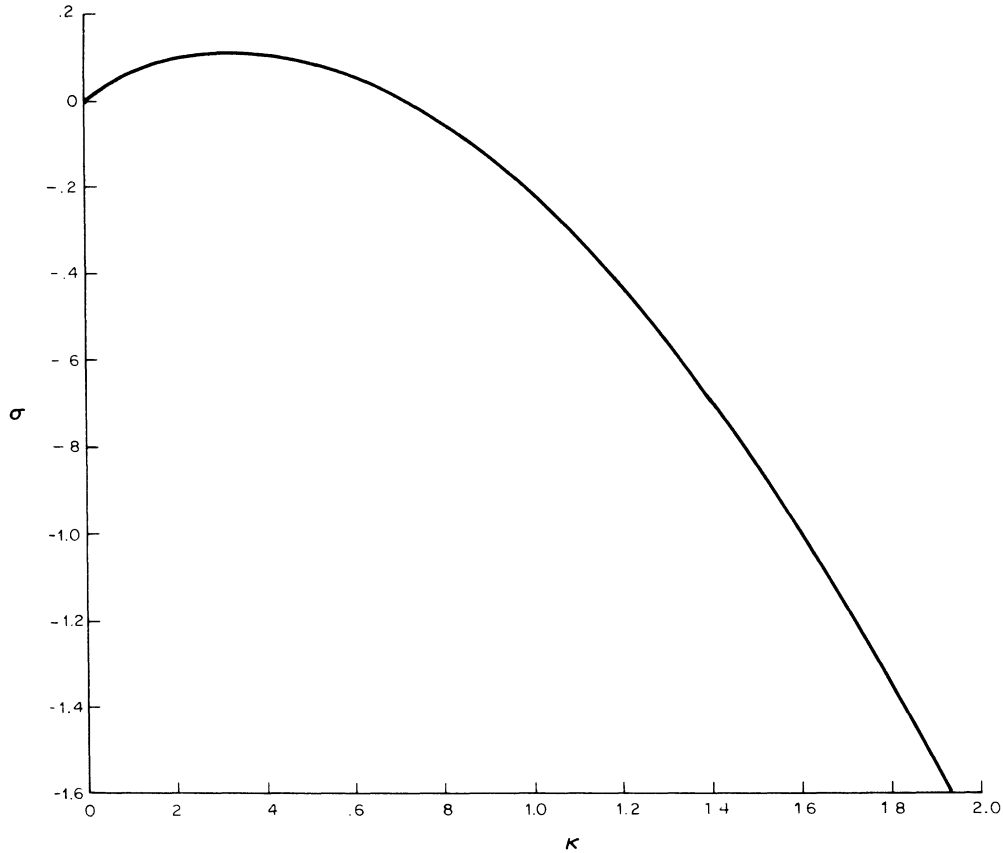


FIG. 8. Surface tension as a function of  $\kappa$ .

As a result of these problems it was difficult to obtain a high accuracy result for what appears to be a relatively simple problem. This is particularly true for large values of  $\kappa$ . Our results for  $\sigma$  are shown in Fig. 8 and we estimate our error to be less than 0.01, which is adequate for our purposes.

The incorporation of surface tension into the bag

model is straightforward and was introduced in its application to QCD by Hasenfratz and Kuti.<sup>14</sup> One simply modifies the pressure balance equation to include the surface-tension pressure, and Eq. (4.2) becomes

$$|B|^2 = 2\sigma(1/r_1 + 1/r_2) - 2E_{\text{vac}}, \quad (4.19)$$

where  $r_1$  and  $r_2$  are the local radii of curvature of the

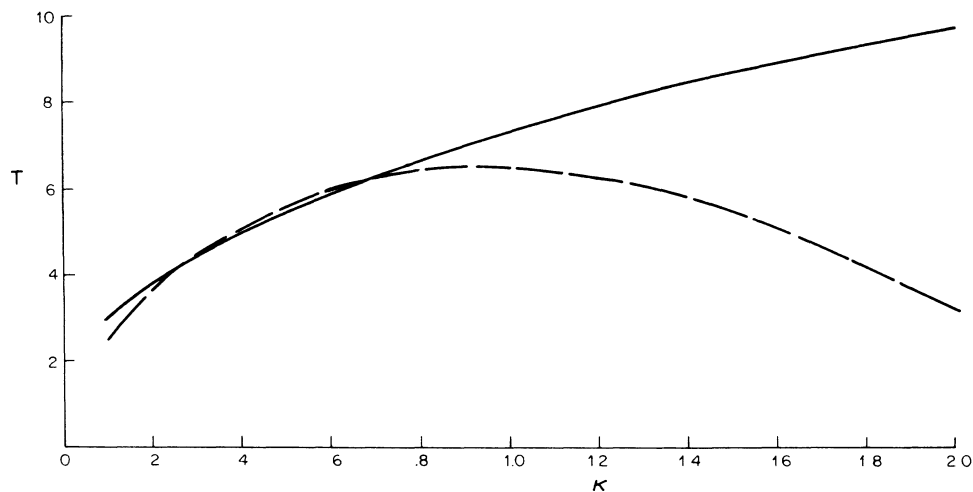


FIG. 9. String tension as a function of  $\kappa$ . LG values are the solid line, while those for the bag approximation including surface tension  $\sigma(\kappa)$  are represented by the dashed line.

surface. The energy also has an extra term  $\sigma S$  where  $S$  is the total surface area. It seems likely that even with the added complication of Eq. (4.19) the bag approximation can be solved, though the analysis of the cusp structure is greatly complicated. For its application to superconductivity,  $\sigma$  is a function of  $\kappa$  which prevents using scaling to remove the  $\kappa$  dependence, meaning that the solutions of Sec. III are actually more easily obtained than those of the bag approximation.

To attempt to determine whether the addition of surface tension will improve the bag approximation results, we note that the major discrepancy can be traced to the incorrect value of the string tension for the simple bag model. For the case of a flux tube, Eq. (4.19) can be combined with the equation for flux conservation to obtain the following equations relating the string tension and the surface tension:

$$8N^2 = \kappa^2 R_N^4 + 2\sigma R_N^3 \quad (4.20)$$

and

$$T_N = \pi(\kappa^2 R_N^2 + 3\sigma R_N) . \quad (4.21)$$

In Fig. 9 we compare the string tension for  $N=1$  calculated from Eqs. (4.20) and (4.21) to that of the Landau-Ginzburg vortex line. Clearly there is considerable improvement in the type-I region. In the type-II region the disagreement is about the same, though the sign of the discrepancy has changed. The fact that the bag approximation string tension is clearly headed toward negative values for large  $\kappa$  is certainly a very unphysical result. In Table I we have given the actual string tension versus the bag approximation string tension as a function of  $N$  for  $\kappa=1$  and  $\sigma = -0.218$ . The discrepancy stays rather constant at about 0.6 scaled units, meaning that the percentage error becomes quite small for a large flux tube, as one might expect. This constant term is what would be obtained if one had a curvature energy per unit area (unit arc length in the string tension) inversely proportional to the radius of curvature. Needless, to say, the bag approximation with surface tension has already lost its computational advantages and further attempts to in-

TABLE I. The string tension for  $k=1$  as a function of units of flux in the vortex line calculated from the Landau-Ginzburg equations and from the bag model with surface tension  $\sigma = -0.218$ .

Units of flux	$T_N$ (LG)	$T_N$ (Bag with surface tension)
1	7.262	6.50
2	15.19	14.44
3	23.34	22.43
4	31.60	30.86
5	39.93	39.19
10	82.22	81.51
15	125.0	124.3
20	168.0	167.4
50	428.6	428.0
100	866.1	865.5

clude curvature energies can only add to its impracticality.

## V. CONCLUSIONS AND DISCUSSION

The monopole-antimonopole interaction energy calculated directly from the Landau-Ginzburg equations appears to be pure Coulomb at short range with a rapid transition to a linear potential at long range. The absence of a transition region with any structure is a behavior previously observed in bag-model calculations of heavy-quark potential. A comparison of the bag approximation with the correct numerical result is in strikingly good agreement for the critical value of the Landau-Ginzburg parameter. It should be noted that at this special value  $\kappa=1/\sqrt{2}$ , many simplifications on the complete theory occur: vortex lines have no interaction; the energy associated with boundaries is zero; in two dimensions the fourth-order system of equations can be reduced to a single second-order equation for a single field. For other values of  $\kappa$  the agreement with the bag calculation is poor but appears to be due to the incorrect value of the string tension given by the bag approximation.

The fact that the changes produced by changing the value of  $\kappa$  seems to be primarily the change of the string tension suggests using the type of scaling used in the bag approximation in which the string tension could be changed, keeping the charges, and hence the short-range Coulomb interaction, unchanged. The scaling that produces this result goes as follows.

Let  $\gamma = T(\kappa_1)/T(\kappa_2)$  then

$$r(\kappa_1) = r(\kappa_2)/\sqrt{\gamma} \quad (5.1)$$

and

$$E(\kappa_1) = \sqrt{\gamma} E(\kappa_2) . \quad (5.2)$$

Using the calculated string tensions and interaction energies at  $\kappa=0.5$ ,  $1/\sqrt{2}$ , and 1, we have plotted the scaled interaction energies in Fig. 10. The fact that these curves are nearly identical, except perhaps for a small  $R$ -independent term, means that this scaling could be used to generate the interaction energies over a large range of  $\kappa$ 's from the string tensions, once the interaction energy for a single value of  $\kappa$  has been calculated.

A further implication of this scaling result is that a bag approximate could have been constructed for each  $\kappa$  if one had simply treated the vacuum energy density in the bag approximation for a free parameter. This means that as a phenomenological model, the bag calculation is quite good, but that the relation between the required bag pressure and the actual vacuum energy density no longer is applicable.

There is one final note concerning our calculations and the limits in which the bag approximation might produce the true interaction energy. For monopoles of high charge, the resulting flux tube has a large radius and there is a rapid transition from the normal state to the superconducting state at the boundary. In the type-I region this certainly seems to be a correct conclusion, in that the surface and curvature energies are small and

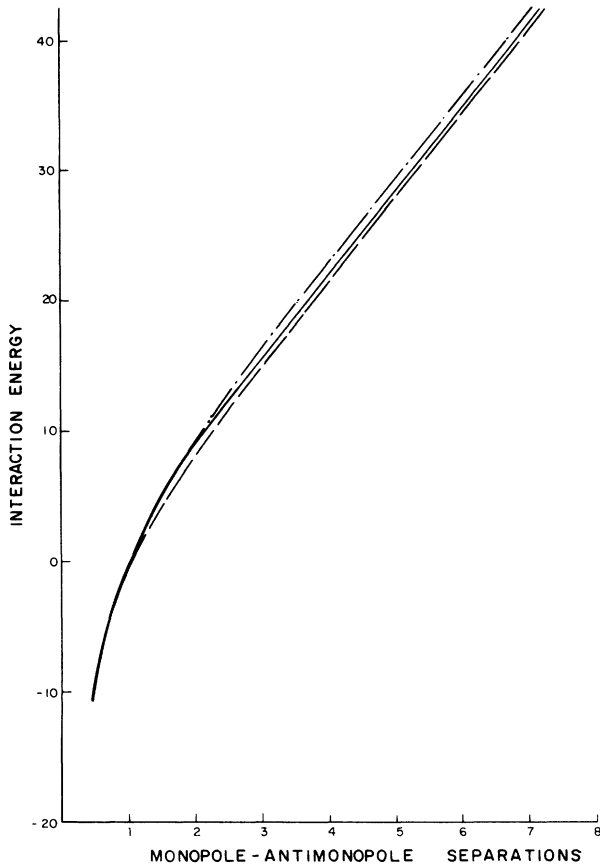


FIG. 10. Scaled LG interaction energies. Solid line is the interaction energy at  $\kappa=0.7071$ . The dashed curve is the LG interaction energy calculated for  $\kappa=1.0$  and scaled via the ratio of the string tensions to  $\kappa=0.7071$ . The dot-dash line is the interaction energy calculated at  $\kappa=0.5$  and scaled via the string tension ratio to  $\kappa=0.7071$ . The small constant difference in the linear portion of the curve probably represents an irrelevant  $\kappa$ -dependent constant.

will certainly be dominated by the volume terms for large values of  $N$ . On the other hand, in the type-II region the minimum energy configuration connecting widely separated monopole-antimonopole pairs is only a single flux tube for  $N=1$ . For all higher values a configuration with  $N$  flux-one tubes will produce a lower string tension than tubes containing higher flux. Thus in a type-II superconductor there is no limit in which one would expect the bag approximation to provide a satisfactory interaction energy.

Clearly the  $N > 1$  monopole-antimonopole interaction in a type-II superconductor lies outside of our assumptions of cylindrical symmetry made in Sec. III. It may be of some interest to see how these nonsymmetric solutions arise from symmetric equations, symmetric sources, and symmetric boundary conditions.

Unfortunately, the scarcity of monopoles prevents any actual experimental test of our calculations, though perhaps the energy required to create macroscopic dipoles in a type-I superconductor could be measured as

well as calculated by our methods.

On the basis of our results we would conclude that the bag model may be a useful tool in treating QCD phenomenology but that the spherical approximation bears little resemblance to the bag shape and that it is unlikely that the bag pressure has much connection with the vacuum energy of the true theory.

We should point out that if one considers a dual superconductor which is simply a LG superconductor with the potential  $A$  replaced by its dual vector potential, our bag approximation is exactly the bag model used in the calculation of the heavy-quark potential. This means that approximating QCD by this type of dual superconductor will lead to the same results as the bag model while perhaps returning more of the physics of QCD.

As phenomenological Lagrangians for QCD are developed, analogous to the Landau-Ginzburg Lagrangian for superconductivity, we would expect more physics to be retained by attempting to simplify these more complicated systems into equations that bear some resemblance to a dual superconductor of the LG type rather than attempting to reduce it to a bag approximation. It is important to note that the cost in computer time for both methods is quite comparable and if the scaling trick is applied to the solutions of Sec. III, the direct numerical result actually is considerably more efficient.

*Note added.* Following the completion of this work, it was brought to our attention that the interaction of magnetic monopoles in a superconductor had been investigated by Wyld and Cutler [H. W. Wyld and R. T. Cutler, Phys. Rev. D **14**, 1648 (1976)], who recognized the relevance of this problem to that of quark confinement. They calculated numerically both the string tension as a function of the Landau-Ginzburg parameter and the force between two monopoles. Both of these calculations are in serious disagreement with our results.

The difference in the string tension is in part traceable to a surface term which they obtained through a by-parts integration. This term, which should have been zero, makes a sizable contribution to their values for the string tension.

In their treatment of the monopole interaction, they chose the string connecting the two monopoles using our expression for  $A_D$  to represent the vacuum value of the vector potential of the monopoles. They then changed variables from  $A$  to  $A_1$  which is, in effect, a gauge transformation so that  $A$  now has strings along the  $z$  axis connecting each monopole to infinity. In this gauge, as in the one we used, the scalar field boundary conditions must change as one approaches the  $z$  axis depending on whether  $A$  vanishes as it does between the monopoles or behaves as  $1/\rho$  as it does for the other portions of the  $z$  axis. In the elliptic coordinates employed by these authors the  $z$  axis between the monopoles is  $\xi=1$  and  $1 > \eta > -1$ , while the other portions of the  $z$  axis are  $\eta = \mp 1$  and  $1 < \xi < \infty$ . The boundary condition imposed in this work appears to be only for  $\xi \rightarrow 1$  and  $\xi \rightarrow \infty$ , but the conditions at  $\eta \rightarrow \mp 1$  for the full range of  $\xi$  seem to be ignored except at the charge locations. Without complete specification of the functions or their normal

derivatives on the boundaries a solution should be impossible. In any case, the formulation used produces singularities which made the numerical treatment more complicated than ours. We believe our results to be correct and can only conclude that either the points discussed above or numerical problems account for the discrepancy. It should be noted that we have the advan-

tage of ten years of computer improvements to simplify our task.

#### ACKNOWLEDGMENT

The research of J.S.B. was supported in part by the National Science Foundation under Grant No. 8405648.

---

<sup>1</sup>H. B. Nielsen and P. Olesen, Nucl. Phys. **B61**, 45 (1973).

<sup>2</sup>Y. Nambu, Phys. Rev. D **10**, 4262 (1974).

<sup>3</sup>S. Mandelstam, Phys. Rev. D **19**, 2391 (1979).

<sup>4</sup>G. 't Hooft, Nucl. Phys. **B190** [FS3], 455 (1981).

<sup>5</sup>V. P. Nair and N. Rosenzweig, Phys. Rev. D **31**, 401 (1985).

<sup>6</sup>M. Baker, J. S. Ball, and F. Zachariasen, Phys. Rev. D **31**, 2575 (1985).

<sup>7</sup>J. W. Alcock, M. J. Burfitt, and W. N. Cottingham, Nucl. Phys. **B266**, 299 (1983).

<sup>8</sup>See, e.g., P. Goddard and D. I. Olive, Rep. Prog. Phys. **41**, 1357 (1978); F. Englert, in *Hadron Structure and Lepton-*

*Hadron Interactions*, Cargèse, 1977, edited by M. Lévy *et al.* (Plenum, New York, 1979), p. 503.

<sup>9</sup>S. Adler and T. Piran, Rev. Mod. Phys. **56**, 1 (1984).

<sup>10</sup>See, e.g., E. L. Burdon and J. D. Faires, *Numerical Analysis*, 3rd ed. (PWS, Boston, 1985).

<sup>11</sup>W. C. Haxton and L. Heller, Phys. Rev. D **22**, 1198 (1980).

<sup>12</sup>M. Baker, J. S. Ball, and F. Zachariasen, Phys. Rev. D **34**, 3894 (1986).

<sup>13</sup>R. Giles, Phys. Rev. D **18**, 513 (1978).

<sup>14</sup>P. Hasenfratz and J. Kuti, Phys. Rep. **40C**, 75 (1978).